

Chapter 2
Literature Review:
Processing, Structural, Mechanical and
Electrochemical Behavior of
Metal Matrix Composites

Chapter 2

Literature Review:

Processing, Structural, Mechanical and Electrochemical Behavior of Metal Matrix Composites

Metal Matrix Composites (MMCs) have high modulus, fracture and compressive strength. They also show improved thermal, wear and corrosion resistance. The characteristics of powder metallurgy processed metal matrix composites are greatly influenced by:

1. Percentage of the reinforcement.
2. Phase and microstructure which depend on the processing parameters and heat treatment schedule.
3. The bonding between the dispersoids and the matrix.

The present chapter briefly reports available literature about the investigations on metal matrix composites (MMCs) describing (i) Processing of composites by powder metallurgy, (ii) aluminium, copper, magnesium and iron based metal matrix composite systems, their structural, mechanical and electrochemical behavior and effect of processing parameters on their properties.

2.1 Manufacture of MMCs by Stir Casting and Powder Metallurgy Process

Large number of processing techniques has been used for the fabrication of metal matrix composites. However, stir casting and powder metallurgy are the two main routes for the preparation of the MMCs and variety of reports on preparation of MMCs by these methods are available in the literature.

Stir casting technique for preparing aluminium-alumina, aluminium-illite (mica) and aluminium-silicon carbide particle composites has been developed by Surappa and Rohatgi (1981). The method essentially consists of stirring uncoated but suitably heat-treated ceramic particles of sizes varying from 10 to 200 nm in molten aluminium alloys (above their liquidus temperature) using the vortex method of dispersion of particles followed by casting of the composite melts. Aluminium-11.8 wt % silicon alloy melts containing γ -alumina, illite clay and silicon carbide particles were poured, at 720°C into rotating cast iron cylindrical moulds of 0.13 m internal diameter and 0.13 m height with a wall thickness of 0.02 m. The speed of rotation of the mould was 800 rpm just prior to pouring and while pouring it was increased to 1000 rpm in about 2 to 3 sec. The mould was spun for 1 min to ensure that solidification of the casting was completed. The solidified castings were sectioned to study the distribution of Al_2O_3 along longitudinal and transverse sections of the casting. It was found from the above discussion that melts of aluminium alloys containing suspended alumina, silicon carbide and illite particles can be permanent mould cast in a variety of shapes with a macroscopically uniform distribution of ceramic particles. On a microscopic scale these ceramic particles are generally present at the grain boundaries in pure aluminium and in hypoeutectic aluminium alloy, these are present in the last frozen inter dendrite regions.

Ilango and Ramakrishnan (1990) reported the composites fabricated from grey cast iron automobile cylinder block boring scrap collected from the automobile industry and Hoganas grade sponge iron powders. These were ball milled in an attrition mill and compacted at a load of 780MPa to form the green compacts. The green compacts were sintered in a tubular furnace at various temperatures, 1050, 1150, 1300 and 1325°C, in hydrogen atmosphere for one hour. Sintering studies were also carried out at a fixed temperature of 1300°C for different times of 15, 60 and 240 min. in hydrogen atmosphere. The effect of temperature on the physical and mechanical properties of the steel sintered for one hour in hydrogen atmosphere was also recorded. The tensile strength and elongation values increase with temperature till

they reach the maximum values of 830 MPa and 5.6%, respectively, at 1300°C. As the sintering temperature rises, the compact density also improves which results in better properties [Liu et al. (1994)]. It has been observed that when the sintering of the metal powder compacts is carried out in an inert atmosphere or reducing atmosphere, the resultant product yields better density and higher dimensional accuracy.

Iron aluminide intermetallics, which exhibit excellent oxidation and sulfidation resistance, were found to be suitable as the matrix phase in metal matrix composites. In particular, ceramics such as TiB₂, ZrB₂, TiC and WC could all be liquid-phase sintered with Fe-40 at% Al iron aluminide [Schneibel et. al (1996)]. Iron aluminide/ceramic composites were produced by mixing pre alloyed Fe-40 at% Al powder with the desired ceramic powder. The whole mixture was poured into an open Al₂O₃ crucible and heating it to a temperature of 1723 K in a vacuum of 10³Pa, holding for 900s at this temperature and finally cooling in the furnace.

Slipenyuk et al. (2006) reported the effect of reinforcement particle size (3 and 14 μm), matrix-to-reinforcement particle size ratio (PSR) ranging from 2.9 to 12.9 and volume fraction of the reinforcement (0–20 vol.%) on microstructure and mechanical properties (yield stress, tensile strength, elongation to fracture and Young's modulus) for Al–6Cu–0.4Mn/SiCp composites manufactured by the powder metallurgy route. The initial powders of the matrix alloy and the reinforcement were blended in a drum mixer (mixing for 1 h in ethanol to reduce the number of particle agglomerates followed by drying and then mixing for 30 h) and cold-compacted into billets with a porosity of 25%. The billets were then canned in aluminum containers, degassed at 400°C and extruded. The formation of the reinforcement clusters in the composites was studied with respect to changes in the reinforcement particle size and volume fraction (under constant particle size of the matrix alloy) as well as upon variation of the particle size of the matrix alloy (for constant reinforcement particle size and volume fraction). It was found that larger reinforcement particles provide higher Young's modulus for equal reinforcement concentration.

The strain gradient theory proposed by Chen and Wang (2002) is of significant importance. He discussed how particle size affects the particle-reinforced metal-matrix composites. Many composite factors, such as the particle size, the particle aspect ratio, the Young's modulus ratio of the particle to the matrix material, particle volume fraction and the strain hardening exponent of the matrix material, are investigated in detail. Two kinds of particle shapes, spheroidal particle and cylindrical particle, are considered to check the dependence of strength on the particle shape. Calculation for the special materials used has been done and the calculation results are consistent with the experimental results.

Tatar and Ozdemir (2010) et al. studied the thermal conductivity of α -Al₂O₃ particulate reinforced aluminum composites (Al/Al₂O₃-MMC) prepared by powder metallurgy method. The thermal conductivity shows linear dependence on temperature in the investigated range. The increase in the thermal conductivity of the composites with decreasing Al₂O₃ particles size was observed which could be due to greater stability of the thermal conductive paths for smaller Al₂O₃ particles. The results show that it is possible to improve the thermal conductivity of the composites with different vol% Al₂O₃. This suggests that alumina particles, conduct heat by phonon and electrons scattering while being electrically insulating. For higher temperature, it can be considered that the jumping probability of electrons through the imperfections becomes saturated and the effect of thermal component becomes more conspicuous on thermal conductivity. As a result, a large number of thermally excited elastic waves (called phonons) scatter conduction electrons and decrease the relaxation time between collisions. It is also seen that the thermal conductivity decreases with increasing Al₂O₃ volume fraction.

Abdizadeh et al. (2011) investigated aluminium – zircon based composites synthesized using powder metallurgy technique. Some green specimens using different volume percentages of zircon were prepared followed by sintering at two different temperatures, 600 and 650°C for 65 min. It was found from the present study that with increasing zircon content of composites, the hardness of specimens

increases to a maximum value of 75 BHN while, increasing temperature facilitates this trend. Also, higher temperatures cause increase in sintered density and relative density up to 92%. Adding more zircon content increases sintered density to 92% but relative density decreases to 86%. Sintering temperature improves mechanical properties like yield stress, elongation and compressive strength. Among all the experiments, specimens sintered at 650°C showed better results than 600°C.

Samal et al. (2013) investigated Cu–graphite metal matrix composites (MMCs) by conventional powder metallurgy route using conventional and spark plasma sintering (SPS) techniques. Cu powders were mixed with graphite to prepare composite powder mixture of 1, 3, 5 and 10 vol. % of graphite. The composite powder mixtures were then cold compacted at a pressure of 700 MPa for 2 min and sintered in tubular furnace at 900°C using argon gas for 1 h. It has been found that addition of graphite into copper does not result in much improvement in the hardness due to soft nature of graphite. However, 90% and 97% of relative density have been obtained for conventional sintered and spark plasma sintered (SPS) samples respectively. Maximum Vickers hardness of around 100 has been achieved for Cu–1 vol. % graphite MMC when it is fabricated by SPS due to the combined effect of pressure and spark plasma effect. However, a hardness value of 65 has been obtained for the same composite when it is fabricated by conventional sintering at 900°C for 1 h. It has been found that the density and hardness of MMCs decreases up to 20 h of milling due to flake formation and increase in size. After 20 hour of milling these values increase as the particle shape becomes irregular and size reduction takes place.

Aluminium-silicon carbide-graphite hybrid composites were prepared using powder metallurgy technique. Tribological properties of the composition Al 2024–5wt%; SiC–x wt% graphite (x=0, 5, and 10) composites were investigated using a pin-on-disc equipment. An orthogonal array, the signal-to-noise ratio and analysis of variance were employed to study the optimal testing parameters using Taguchi design of experiments. The analysis showed that the wear loss increased with increasing sliding distance and load but was reduced with increased graphite content. The

coefficient of friction increased with increasing applied load and sliding speed. The composites with 5 wt% graphite had the lowest wear loss and coefficients of friction because of the self-lubricating effect of graphite. Conversely, due to the effect of the softness of graphite, there was an increase in wear loss and the coefficient of friction values in composites with 10 wt% graphite content. The morphology of the worn-out surfaces and wear debris was examined to understand the wear mechanisms. The wear mechanism is dictated by the formation of both delamination layer and mechanically mixed layer (MML). The overall results indicated that aluminium ceramic composites can be considered as outstanding materials where high strength and wear-resistant components are of major importance, particularly in aerospace and automotive engineering sectors [Ravindran et al. (2013)].

2.2 Aluminium Based Metal Matrix Composite

Critical need for high strength, lightweight and high stiffness materials has resurrected much interest in discontinuously reinforced powder metallurgy processed metal matrix composites. These hybrid materials use both standard wrought alloys of aluminium and a wide variety of discontinuous reinforcements such as particulates and whiskers of ceramic materials [Surappa and Rohatgi (1981); Srivatsan et al. (1991)]. Renewed interest in these materials as attractive candidates for use in the aerospace and transportation industry has resulted from an attractive and unique combination of physical and mechanical properties and an ability to offer near isotropic properties coupled with their low cost as compared with existing monolithic materials. The variables involved in each processing technique are carefully examined and its influence on the alloy chemistry is highlighted. Novel processing techniques for these materials such as the variable co-deposition method is presented as a means to process these novel engineering materials in order to improve their overall mechanical performance.

During the past decade, considerable research efforts have been directed towards the development of in situ metal matrix composites (MMCs) especially using aluminum

as the matrix phase in which the reinforcements are formed in situ by exothermic reactions between elements or between elements and compounds. Using this approach, MMCs with a wide range of matrix materials and second-phase particles have been produced. Because of the formation of ultrafine and stable ceramic reinforcements, the in situ MMCs are found to exhibit excellent mechanical properties. Current development on the fabrication, microstructure and mechanical properties of the composites reinforced with in situ ceramic phases is an important investigation. Particular attention is paid to the mechanisms responsible for the formation of in situ reinforcements and for creep failure of the aluminum-based matrix composites [Tjong and Ma (2000)].

Rahimian et al. (2009) reported Al-Al₂O₃ composites synthesized via powder metallurgy technique. The investigation focused on the effect of alumina particle size, sintering temperature and sintering time on the properties of composite. The average particle size of alumina was 3, 12 and 48µm (Fig. 2.1). Sintering temperature and time were in the range of 500–600°C and 30-90 min. Fig. 2.2 and 2.3 show the effect of sintering time (45, 60 and 90 min at 600°C) and sintering temperature (500, 550 and 600°C for 45 min) on the microstructure of the composites. The amount of densification increases as the sintering time increases from 45 to 90 minutes. It is seen that at higher sintering temperatures, a denser structure is formed due to higher diffusion rates. The manifestation of the evolution of microstructure with sintering temperature can clearly be seen by the changes in the morphology and the size of the grains and pores.

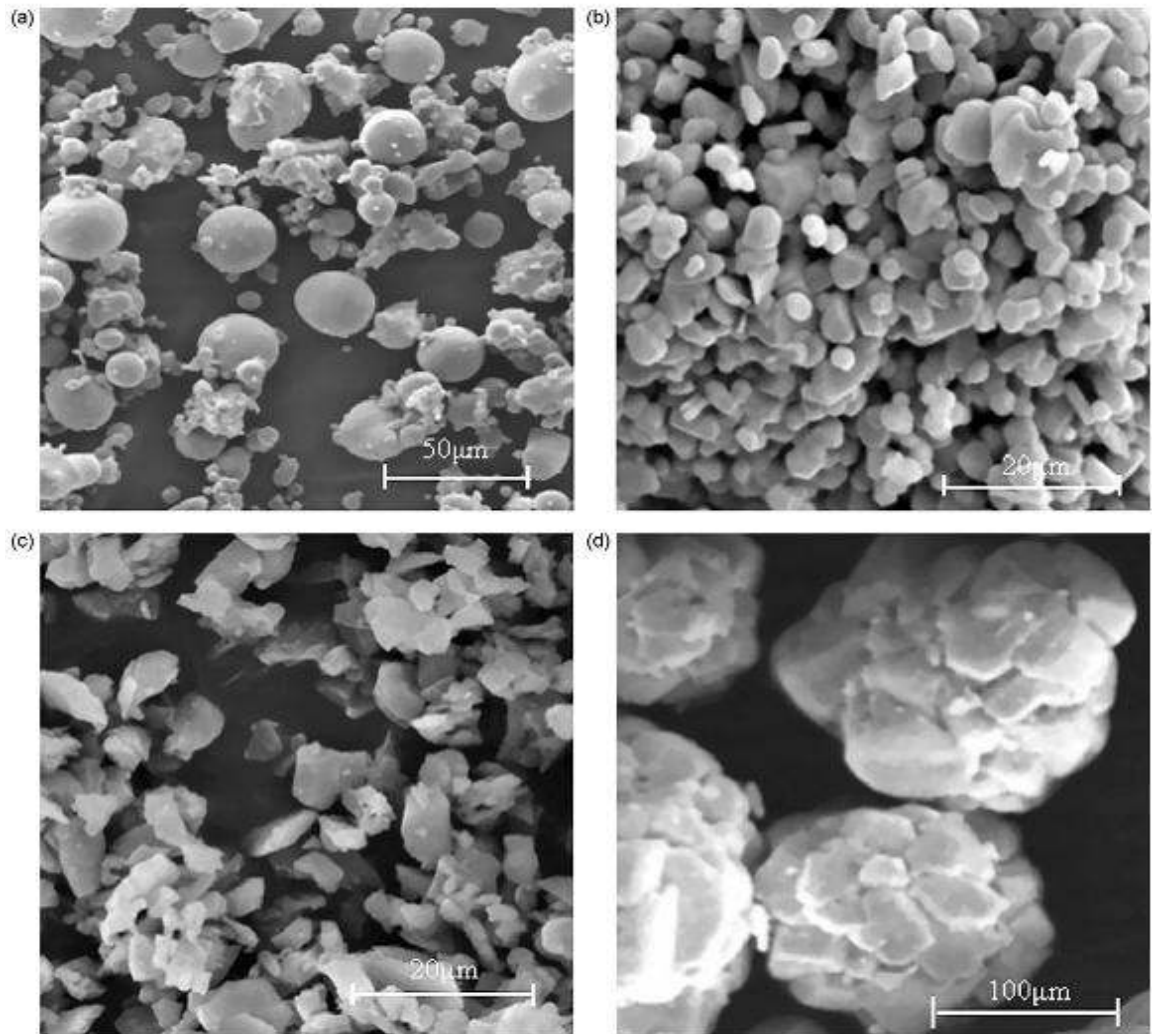


Fig. 2.1 SEM micrographs of Al and Al₂O₃ powders (a) Al (b) Al₂O₃-3 μm (c) Al₂O₃-12 μm and (d) Al₂O₃-48 μm [Rahimian et al. (2009)]

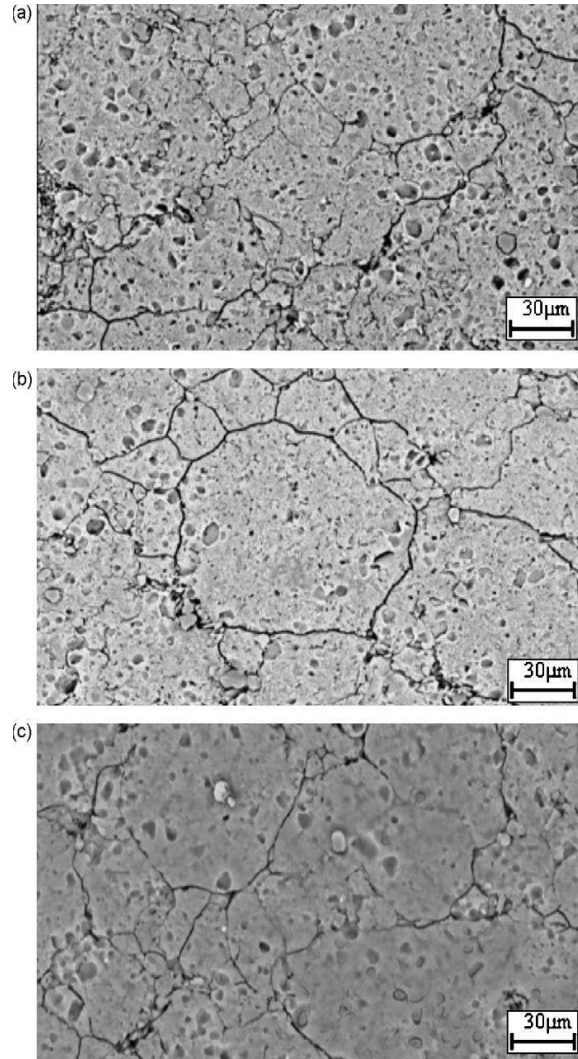


Fig. 2.2 Effect of sintering time on microstructure of composites at 600°C (a) 45(b) 60 and (c) 90 min [Rahimian et al. (2009)]

A correlation is established between the microstructure and mechanical properties. The investigated properties include density, hardness, microstructure, yield strength, compressive strength and elongation at fracture. It has been concluded that as the particle size of alumina is reduced, the density is first increased followed by a fall in density. In addition, for low particle size, the hardness, yield strength, compressive strength and elongation at fracture were higher as compared to coarse particles. The variation in properties of Al-Al₂O₃ composite is dependent on both the sintering temperature and time. Prolonged sintering times had an adverse effect on the strength of the composite.

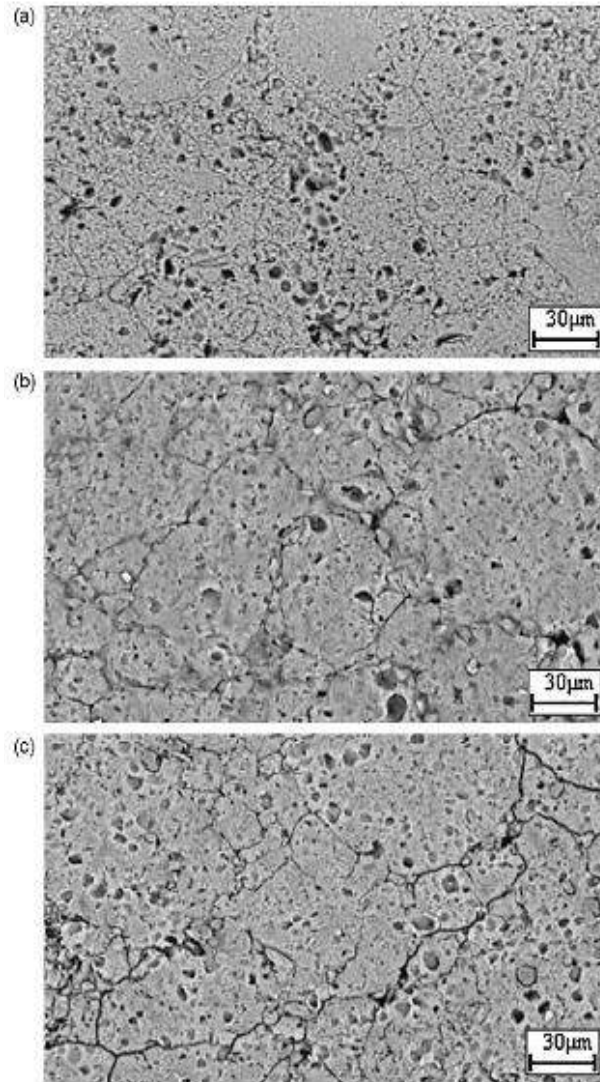


Fig. 2.3 Effect of sintering temperature on microstructure of composites after sintering for 45 min (a) 500, (b) 550 and (c) 600°C [Rahimian et al. (2009)]

Rabiei et al. (2008) investigated the aluminum matrix composites with various particle reinforcements experimentally to evaluate the fracture toughness. The experimental results have been compared with the fracture toughness estimates using the Hahn–Rosenfield model. It is observed that the Hahn–Rosenfield model has a validity range for reinforcement particle sizes of 5-10 μm . A modification of this model has been developed for estimating the fracture toughness of the metal matrix composites with larger particle reinforcements. The validity of the modified model has been experimentally tested. There has been a close agreement between the

experimental results and the predicted toughness using the modified fracture model [Tahamtan et al. (2013)].

Trzaskoma et al. (1983) reported the effect of SiC phase on the corrosion behavior of SiC/Al metal matrix composites in 0.1 and 0.6 N NaCl both in the presence and absence of dissolved oxygen. Anodic polarization behavior has been studied and pitting potentials have been measured for three composite systems: SiC/Al 2024, SiC/Al 6061, and SiC/Al 5456. General corrosion behavior and the effects of anodizing on the corrosion resistance of the composites have been studied by a-c impedance techniques. The results show that pitting susceptibility is about the same for the composites and their corresponding alloys, except for Al2024. In this system, the composite is less resistant to pit initiation than the corresponding wrought aluminum alloy. General corrosion is more significantly affected by the presence of oxygen than by the SiC phase. In the absence of oxygen, corrosion resistance is improved for both the alloys and composites. In addition, the corrosion resistance of the composites can be improved by anodizing.

The corrosion resistance of an Al 6092/W, metal matrix composite (MMC) has been evaluated by recording the impedance spectra during immersion in 0.5 N NaCl for at least one week [Chen and Mansfeld (1997)]. Various methods of corrosion protection were applied in his experiments. These included surface modification in the Ce-Mo process and anodizing in sulfuric acid. Anodized surfaces were sealed by immersion in hot water, cerium nitrate and two different dichromate solutions. Significant improvements of the corrosion resistance were only observed for the surface anodized with a dichromate seal. Considerable corrosion mainly in the form of pitting occurred for the untreated Al 6092/SiC, MMC during exposure to 0.5 N NaCl for seven days. The Ce-Mo process which has been applied successfully for Al 2024, Al 6061 and Al 7075 did not provide additional corrosion protection. Anodizing followed by hot water sealing also did not increase the corrosion resistance of the MMC. Sealing in $\text{Ce}(\text{NO}_3)_3$, which is a component of the Ce-Mo process, provided better results than

sealing in hot water, however, a few pits still initiated in a short time. Sealing in dichromate eliminated pitting during immersion in 0.5 N NaCl for two weeks. Unfortunately, due to environmental concerns, this type of sealing was abandoned.

Lozano et al. (2007) investigated the corrosion characteristics of Al/SiCp/spinel composites fabricated with SiCp, fly ash (FA) and recycled aluminum. For type A composites prepared with the alloy Al–8Si–15Mg (wt.%), the Mg₂Si intermetallic precipitated during solidification acted as a micro anode coupled to the matrix (in the presence of condensed humidity) and led to catastrophic localized corrosion. Although the potential attack of SiC by liquid aluminum was successfully avoided by the presence of SiO₂ in the FA, Al₄C₃ still formed due to the reaction of carbon in the FA with aluminum. For type B composites, processed with the alloy Al–3Si–15Mg (wt.%) and calcinated FA, the silicon content was low enough to avoid formation of Mg₂Si. Moreover, chemical degradation by Al₄C₃ hydrolysis did not occur either because of the absence of carbon or due to the presence of SiO₂. This explains the physical integrity of type B composites even after 11 months of exposure to humid environment. By using calcined fly ash, the chemical degradation of the composites is fairly avoided.

He et al. (2011) reported the corrosion behavior of anodized coating on 2024 aluminium and SiC particles reinforced 2024 aluminium metal matrix composites in 3.5 wt% NaCl aqueous solution using electrochemical methods. The results show that the anodized coating on 2024Al provides good corrosion protection to 3.5 wt.% NaCl and the anodized coating on the SiCp/2024Al MMC provides some corrosion protection, but it is not as effective as for 2024Al because of non-uniformity in thickness and cavities associated with the SiC particulates. Cavities above SiC particles are the reason that the anodized coating on the MMC cannot be completely sealed by hot water as with anodic Al alloy. SiC particle anodizes at a significantly reduced rate compared with the adjacent Al matrix. This gives rise to alumina film encroachment beneath the particle and occlusion of the partly anodized particle in the coating. It was found that the barrier layer of anodized Al MMC is not continuous and

it is composed primarily of the barrier layer of anodized Al matrix and a barrier-type SiO₂ film on the occluded SiC particles in the coating. New formation mechanisms of coating growth during anodizing of a SiCp/2024Al MMC were proposed.

2.3 Copper based Metal Matrix Composites

The other material which has potential as the matrix phase is copper. Dispersion-strengthened copper has the ability to retain most of its properties at elevated temperatures. Among various processes, the powder metallurgy preparation route is ideal because of its efficient dispersion of fine particles. Copper composites containing 0-3 wt% Al₂O₃ were sintered in hydrogen atmosphere at 800°C-900°C. The powders were prepared through the blending and mechanical alloying routes. The compaction pressures used were 500 and 560 MPa respectively. With an increase in compaction pressure, both sintered density and hardness increased. It was found that densification was faster for mechanically alloyed powder compacts than the blended ones. An increase in Al₂O₃ content in general increased hardness with an increase in associated loss in electrical conductivity [Upadhyaya and Upadhyaya (1995)].

Moustafa et al. (2002) reported about the copper matrix composites reinforced with either Ni-coated or uncoated SiC and Al₂O₃ particulates synthesized by powder metallurgy technique. The reinforcement particles of SiC and Al₂O₃ were coated with a thin layer of nickel by electroless method. The coated or uncoated reinforcement particles of either SiC or Al₂O₃ were added to copper metal powders with nominal loading of 20 wt.% mixed in a mechanical mixer having 360 rpm for a period of 10 min. Each mixture of the investigated powders was cold compacted at 600 MPa and sintered at 900°C in hydrogen atmosphere. Figs. 2.4(a) and (b) show micrographs of Ni-coated SiC and Ni-coated Al₂O₃ powders. The coating procedure used in this study resulted in a batched Ni-precipitation on the surfaces of either SiC or Al₂O₃ particles. The phosphorous concentration was very limited and it was less than 0.03%. The microstructures developed in the sintered composites reveal the differences in their processing parameters.

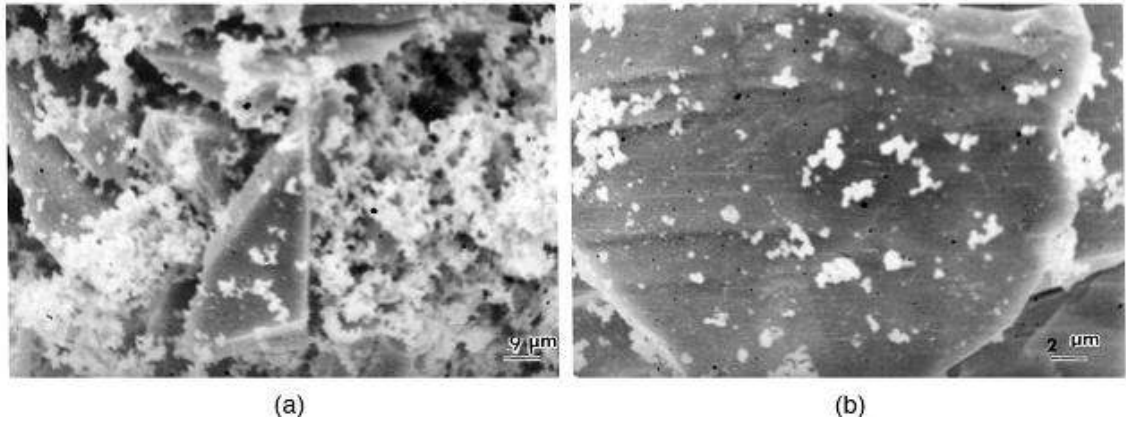


Fig. 2.4 Micrographs of powders of: (a) Ni-coated SiC, (b) Ni-coated Al₂O₃ [Moustafa et al. (2002)]

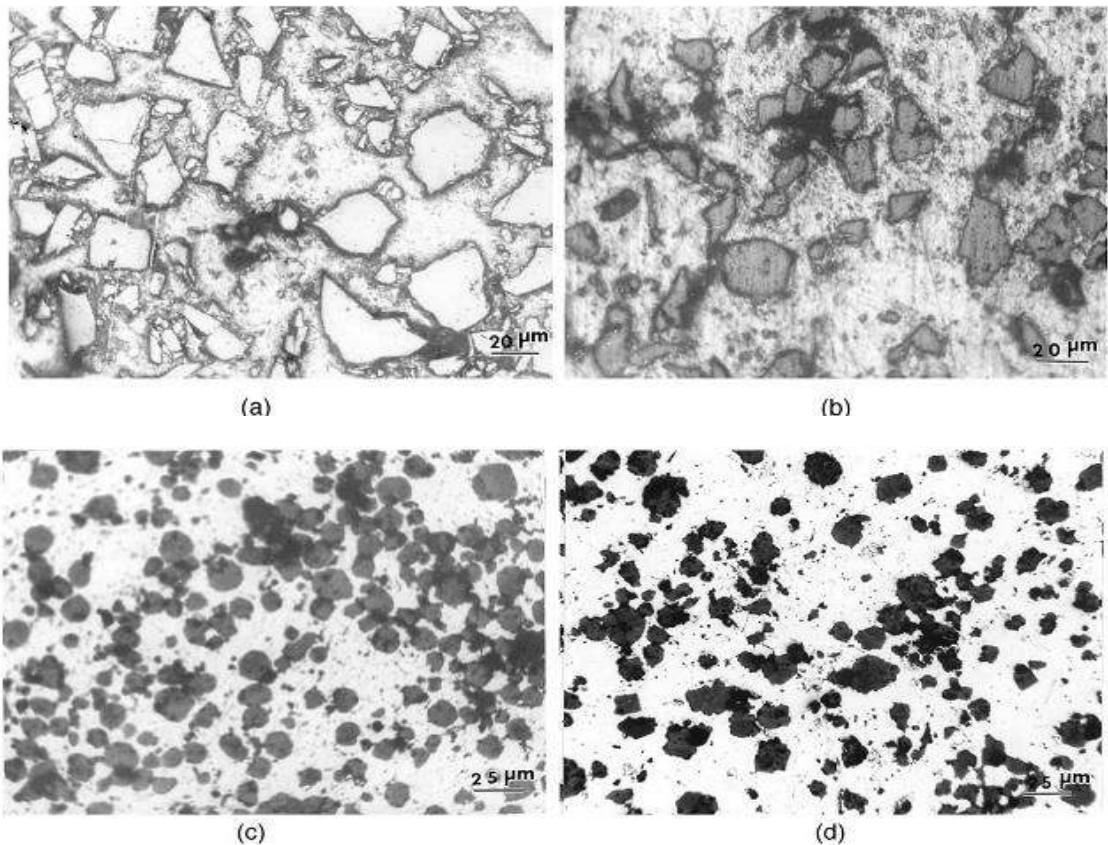


Fig. 2.5 Microstructures of: (a) Cu-20% coated SiC (b) Cu-20% SiC (c) Cu-20% coated Al₂O₃ and (d) Cu-20% Al₂O₃ composites [Moustafa et al. (2002)]

Figs. 2.5(a-d) show micrographs of Cu-20% coated SiC, Cu-20% SiC, Cu-20% coated Al₂O₃, and Cu-20% Al₂O₃ composites respectively. Fig. 2.5(a) shows a very good adhesion between SiC particles and Cu-matrix but uncoated SiC micrograph i.e.

Fig. 2.5(b) shows that the adhesion between SiC particles and Cu-matrix is poor due to presence of gaps and porosity between SiC and Cu-matrix. Almost no detectable porosity and very good adhesion between particles and Cu-matrix is observed in Cu-coated Al₂O₃ composite as indicated in Fig. 2.5(c). In the case of Cu-uncoated Al₂O₃ composite i.e. Fig. 2.5(d) gaps between Al₂O₃ particles and Cu-matrix are observed. Metallographic observation of the composites produced by uncoated reinforcement of both SiC and Al₂O₃ shown in Fig. 2.5(b) and (d), revealed that both closed and interconnected porosity is present.

The presence of porosity in the case of Cu-uncoated reinforcement composites could be attributed to the full or partial masking of Cu powder with fine dust of SiC or Al₂O₃ which was generated during the mixing process of uncoated reinforcement and Cu. During sintering, the Cu/Cu contacts became less, but SiC/SiC or Al₂O₃/Al₂O₃ contacts increased due to partial covering of Cu powder with reinforcement dust. This resulted in weak interfacial bonding between SiC or Al₂O₃ and Cu-matrix. The yield stress measured was 0.2% proof stress for all composites. It was noticed that all compressed samples, either coated or uncoated, fractured at an inclined angles of 45° which means that fracture is taking place by a shear mode. The results compiled in Table 2.1 demonstrate that the yield and breaking (fracturing) strengths of the coated composites are much higher than those of uncoated composites. Also, it was noted that the compressive strains of coated composites are more than those of uncoated composites. The improvements of compression properties of the coated composites could be attributed to the good adhesion between coated particles and the Cu-matrix, in addition to the higher density and lower porosity [Moustafa et al. (2002)].

Table 2.1 Compression properties of: Cu–20% coated SiC, Cu–20% SiC, Cu–20% coated Al₂O₃, and Cu –20% Al₂O₃ composites [Moustafa et al. (2002)]

Materials composition	0.2% proof stress (MPa)	Fracture strength (MPa)	Elongation (%)
Cu–20% coated SiC	83	344	43.6
Cu–20% SiC	16	135	30.4
Cu–20% coated Al ₂ O ₃	62	285	48.4
Cu–20% Al ₂ O ₃	14.1	112	33.2

Luo et al. (2007) investigated SiC fiber reinforced copper matrix composites prepared by foil-fiber-foil method (FFF) and, fiber-coating method (MCF) with and without a Ti6Al4V interlayer. The copper coating was prepared by different electroplating processes and the Ti6Al4V interlayer by magnetron sputtering. The results showed that the tensile strength of the specimens without Ti6Al4V interlayer was nearly identical and poor, between 250 and 290 MPa. The specimen with Ti6Al4V interlayer exhibited tensile strength over 500 MPa. This great increase was attributed to the improvement of the SiC/Cu interfacial bonding strength because the interfacial reactions occur at Cu/Ti6Al4V interface and Ti6Al4V/SiC interface. Additionally, there are generally many micro pores produced by hydrogen and oxygen in the electroplated coating which would influence the density of the matrix. Therefore, the densification of the matrix was worth investigating since it would influence the thermal and electrical conductivity of the composite, though it has only a little contribution to the tensile strength. Experiments indicate that proper heat-treatment before hot pressing could improve the densification of the matrix.

Palta et al. (2012) investigated the effect of Cu addition on the wear and corrosion properties of “in situ” Mg₂Si particle reinforced Al–12Si–20Mg matrix composites produced with help of the nucleation and growth of the reinforcement from the source matrix in order to overcome the disadvantages of composites produced by externally reinforcing ceramic particles. Composites such as Al–12Si–20Mg–XCu were produced by adding 1%, 2%, and 4% Cu, to the Al–12Si–20Mg alloy in order to

achieve this purpose. The microstructural characterization, hardness, wear and corrosion properties of composites were correlated and analyzed. Wear experiments under dry environment for alloys using a pin-on-disc type wear device under different loads and at different sliding distances were carried out. Fig. 2.6 shows the effect of sliding distance on the weight loss of the investigated alloys at (a) 3 N (b) 5 N and (c) 20 N loads.

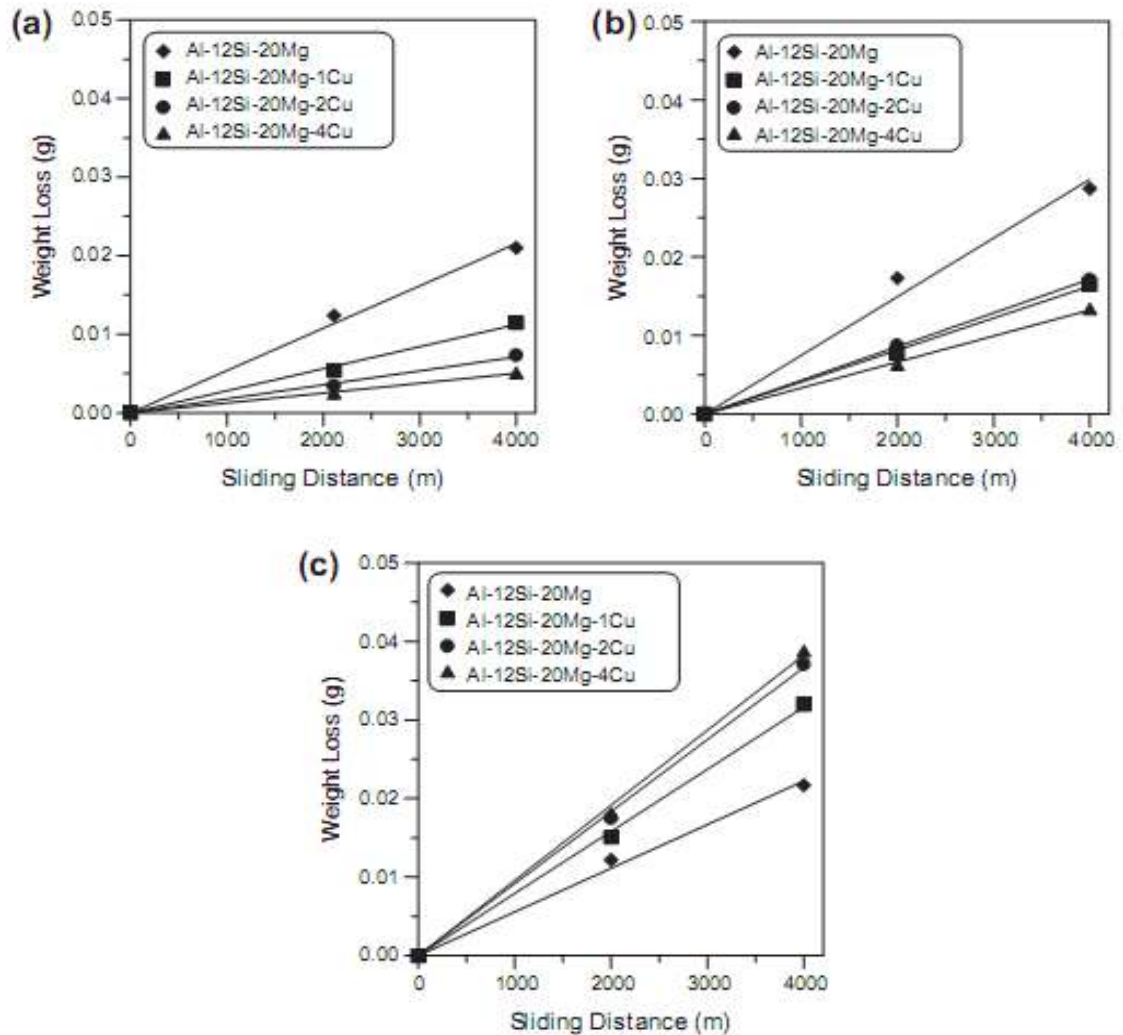


Fig. 2.6 The effect of sliding distance on the weight loss of the investigated alloys (a) 3 N (b) 5 N and (c) 20 N [Palta et al. (2012)]

The weight loss in test specimens under the action of solution containing 30 g/l NaCl + 10 ml/l HCl, and the tafel extrapolation method were used to analyze corrosion behavior of these composites. Results of microstructural characterization concluded

that as the amount of Cu added to the Al–12Si–20Mg alloy increased, the size and volume of the Mg₂Si particles formed within the matrix decreased and CuAl₂ intermetallics formed in the matrix. Results of the wear experiments showed that addition of Cu developed wear resistance under small loads and reduced wear resistance under high loads. According to the results of corrosion experiment, corrosion resistance increased with the addition of Cu. Fig. 2.7 shows SEM micrographs of the worn surfaces of the investigated alloys.

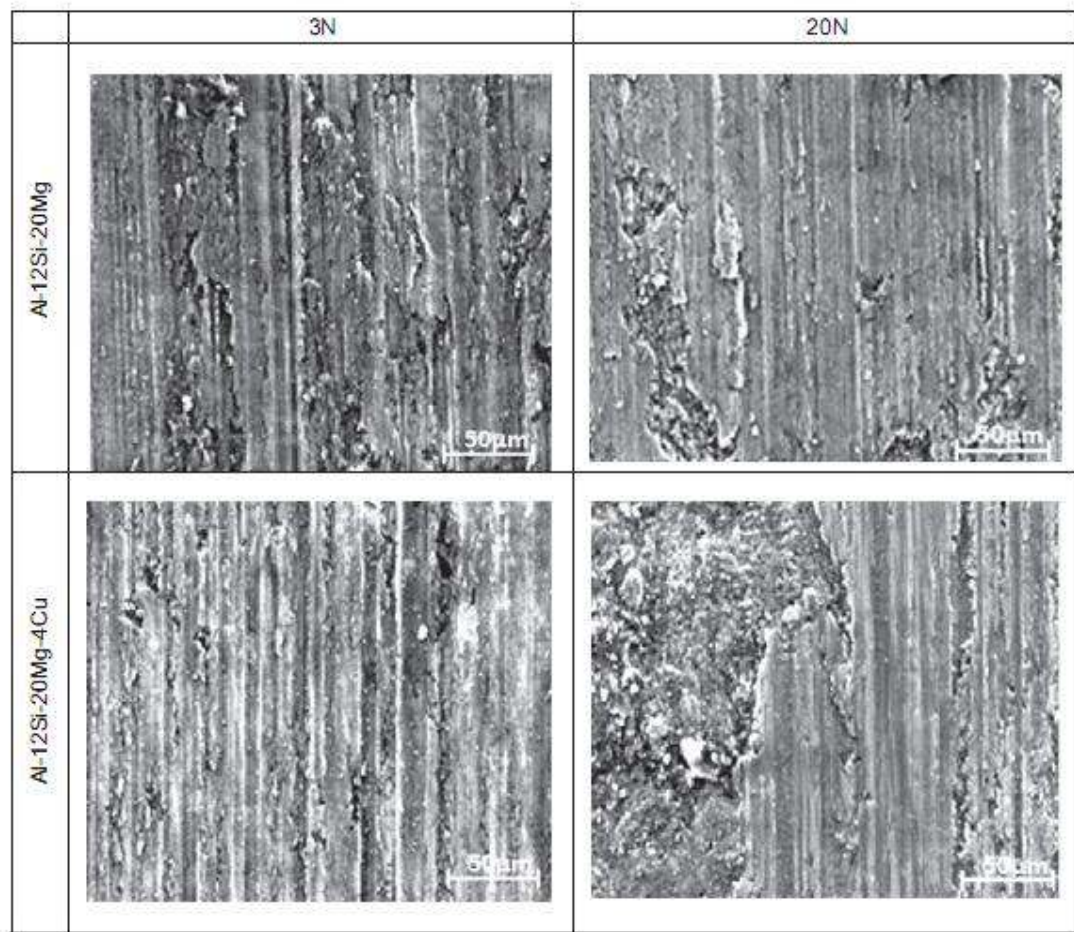


Fig. 2.7 SEM micrographs of the worn surfaces of the investigated alloys [Palta et al. (2012)]

2.4 Magnesium based Metal Matrix Composites

Xiuqing et al. (2005) investigated magnesium matrix composite reinforced with 3.9 vol.% (TiB₂+TiC) particulate which was in-situ synthesized using remelting and

dilution (RD) technique successfully. The process comprised of three steps. These were; (i) synthesis of activated powder, (ii) its sintering and dilution and (iii) remelting of sintered block in molten magnesium. In the experiment, the powder of Al, Ti and B₄C with purity upto 99.5% and size less than 75 μm were used as the base materials of sintered block at first. The composition of the powder mixture being 50% Al, 36.4% Ti and 13.6% B₄C by weight was milled in which the ratio of ball and powder was 5:1 and the milling time was 5 h. The mixed powder was pressed into a block 30 mm diameter and 50 mm height under 15 MPa pressure.

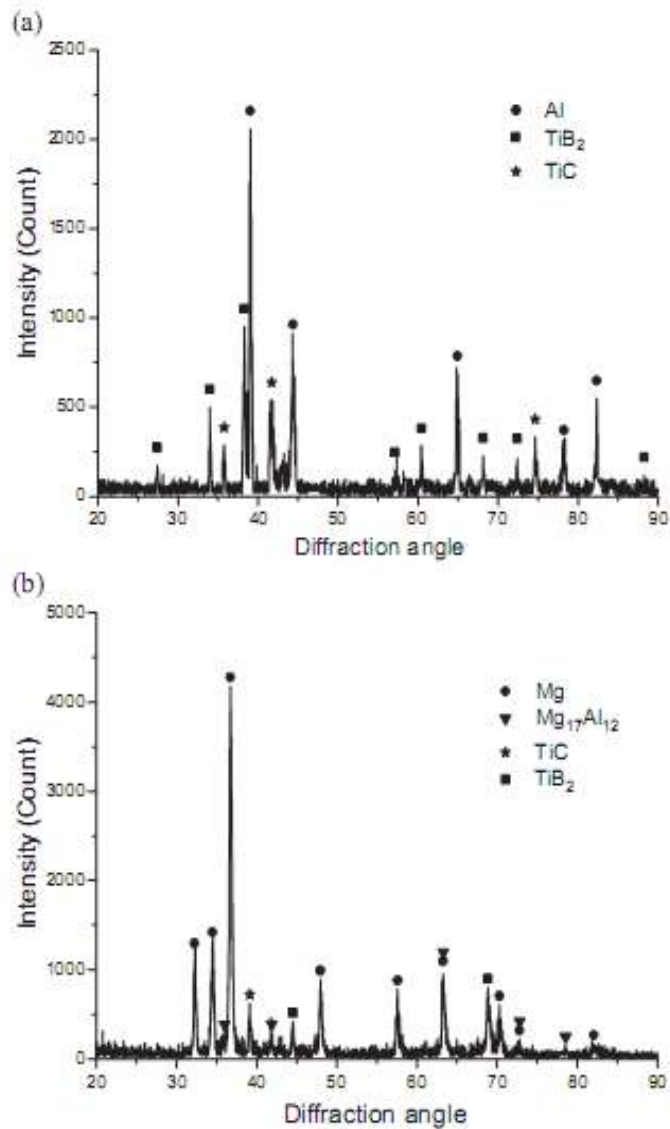


Fig. 2.8 XRD patterns of samples (a) sintered block, (b) magnesium matrix composite [Xiuqing et al. (2005)]

The relative density of blocks was about 50–70%. Then, the blocks reacted at 1400 K for 20 min in Ar gas atmosphere protection. X-ray diffraction (XRD) analysis and microstructural characterization of the sintered blocks revealed the formation and uniform distribution of fine reinforcements.

Fig. 2.8 shows the XRD patterns of samples (a) sintered block and (b) magnesium matrix composite. XRD results revealed the presence of Al, TiB₂ and TiC phase in the sintered blocks and the presence of Mg, TiB₂, TiC and Mg₁₇Al₁₂ phases in Mg/(TiB₂+TiC) composite. Microstructural characterization and energy dispersive spectroscopy (EDS) analysis of the composite material revealed retention and uniform distribution of fine reinforcement. Fig. 2.9 shows SEM photograph of samples (a) sintered blocks and (b) magnesium matrix composite.

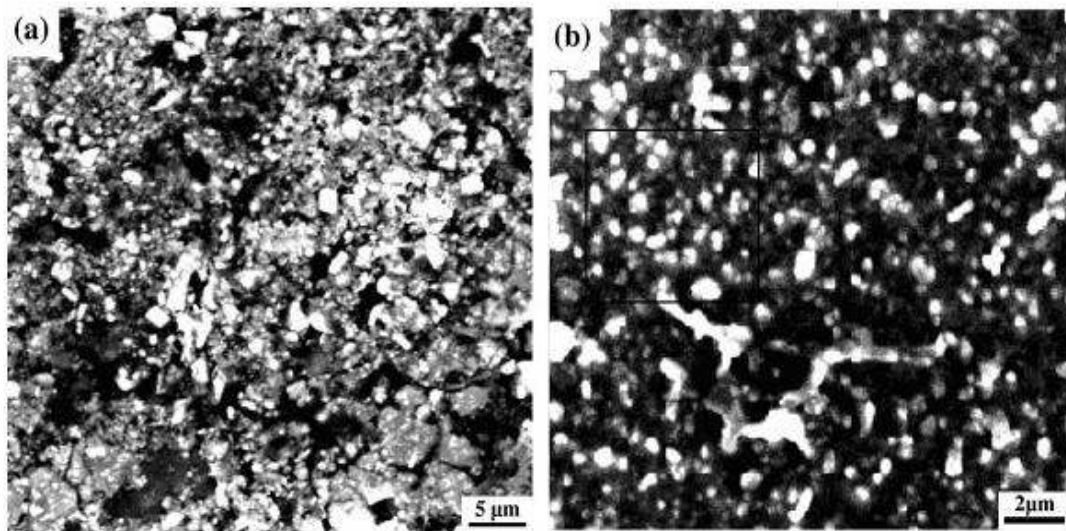


Fig. 2.9 SEM photograph of samples (a) sintered blocks, (b) magnesium matrix composite [Xiuqing et al. (2005)]

Chua et al. (1999) reported AZ91 (Mg₉Al_{0.7}Zn_{0.15}Mn) magnesium alloy reinforced with different sizes of SiC particulates fabricated using powder metallurgy route. Mg, Al, Zn, Mn powders and SiC particulates were mixed in a double cone blender at a rotation speed of 50 rpm for 1 h. After mixing, the powder mixture was cold compacted to a size of 40 mm height and 35 mm diameter. The green compact was heated at 400°C for 30 min followed by extrusion. SEM micrographs in Fig. 2.10

show the composites reinforced with the different sizes of SiC in the transverse direction. Although some agglomeration of SiC particles could be observed, the distribution generally appeared to be reasonably homogeneous. Mechanical properties of the specimens have been studied. Yield and ultimate tensile stress show a decrease with increase in the size of SiC particulates. The influence of thermal shock between 30°C and 400°C on the mechanical properties was also investigated. The results show a decrease in yield stress and elongation at fracture with the number of thermal shock cycles. Table 2.2 illustrates mechanical properties of composites reinforced with SiC of different sizes.

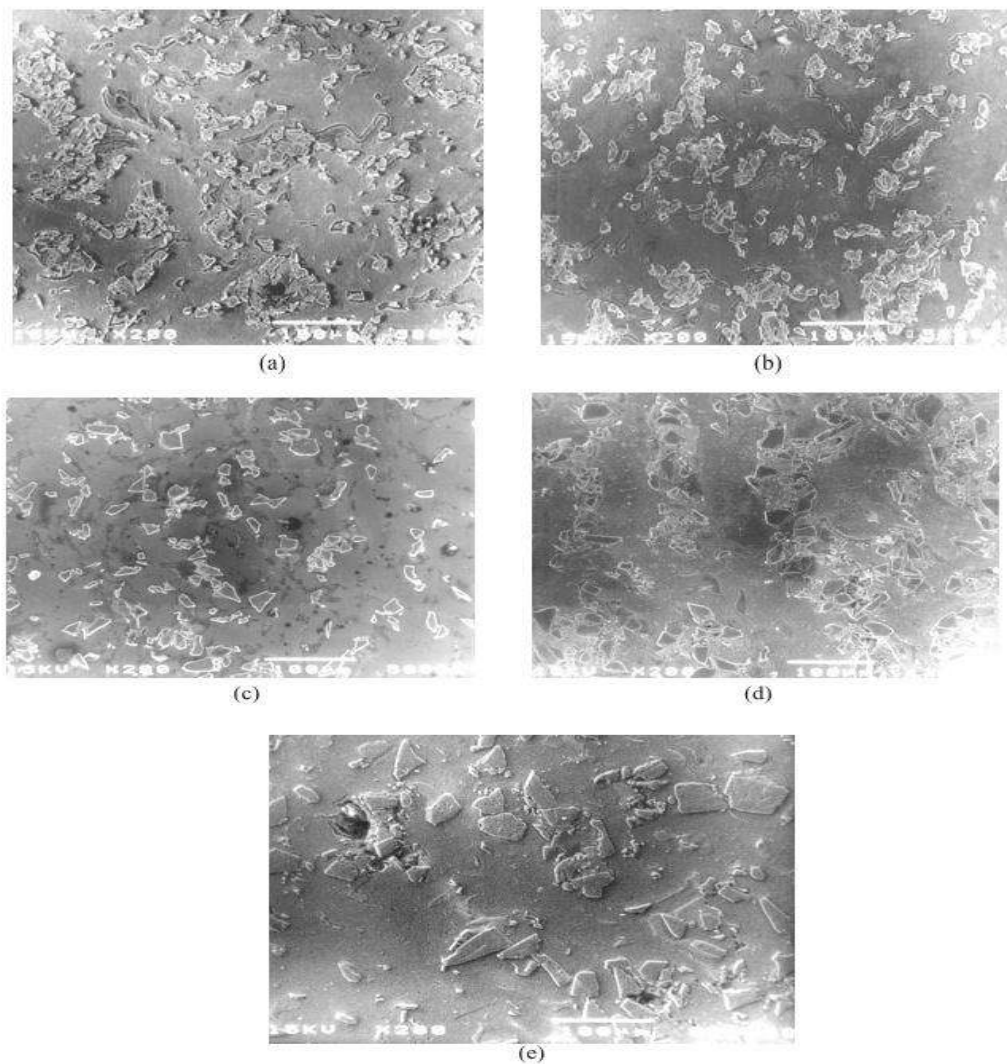


Fig. 2.10 SEM micrographs of Mg matrix composite (transverse direction) reinforced with SiC of size: (a) 15, (b) 20, (c) 25, (d) 38 and (e) 50 μm [Chua et. al. (1999)]

Table 2.2 Mechanical properties of composites reinforced with SiC of different sizes [Chua et al. (1999)]

Size of SiC (μm)	0.2% YS (MPa)	Elastic Modulus (GPa)	UTS (MPa)	Elongation (%)	Predicted fracture toughness, K_{IC} (MPa $\text{m}^{1/2}$)
Matrix alloy	150.00	42.00	190.00	1.15	–
15	120.00	44.50	135.00	0.47	17.70
20	117.00	45.10	120.00	0.24	19.38
25	117.50	42.15	127.50	0.33	21.60
38	110.00	42.00	120.00	0.45	25.80
50	105.00	49.80	110.00	0.23	9.75

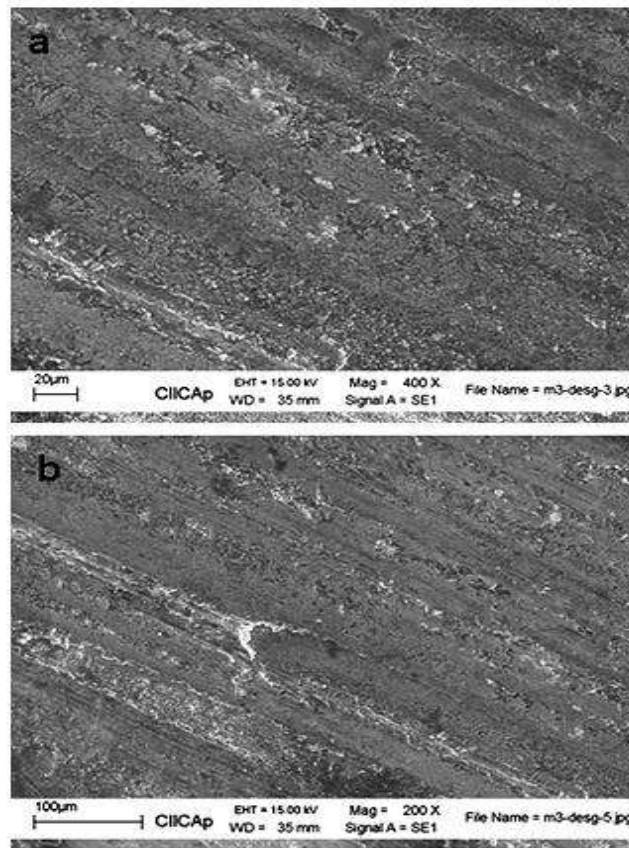


Fig. 2.11 SEM of (a) Worn surface of the alloy showing oxide formation (b) Worn surface of the alloy with oxides agglomeration [Franco et al. (2011)]

Franco et al. (2011) reported metallic matrix composites (MMC) fabricated using Mg-AZ91 alloy and TiC as reinforcement via pressureless infiltration technique. The composites were worn against different AISI 4140, AISI 1045 and H13 steel discs. Wear resistance was evaluated under dry sliding condition at different loads. Chemical analyses of worn out sample shows the formation of different oxides

corresponding to the elements present in the composite during the test. Generalized wear mechanisms of the composites are basically of the type abrasion–adhesion. The wear resistance in all the cases was better in the MgAZ91E alloy than in the composite MgAZ91E/TiCp.

The results indicated that the wear resistance of the Mg AZ91 alloy presents a positive behavior when the pin sample are worn over the AISI 4140 steel and the worst when the steel was AISI H13. Therefore, at this TiC particulate concentration, the composite presents favorably a low response for the automotive applications, since the obtained wear rates are higher in comparison with the unreinforced alloy. It is concluded that the resistance of the material is not enough to support the applied load on the brake and TiC particles depletion occurs. They were working to reduce the particulate concentration in the MMC's. Fig. 2.11 illustrates SEM of (a) Worn surface of the alloy showing oxide formation (b) Worn surface of the alloy with oxides agglomeration.

Deng et al. (2012) studied three kinds of magnesium matrix composites reinforced by SiC_p having size of 0.2, 5 and 10 μm respectively fabricated by stir casting technology. The as-cast ingots were deformed by the combination of forging and extrusion process. Typical microstructures were obtained in the composites reinforced with different particle size. For the composites with lower volume fraction of particles (2%), submicron SiC_p had significant influence on grain refinement and strengthening effect. This resulted in better mechanical properties of submicron SiC_p/AZ91 composite [Ma et al. (2005)]. However, mechanical properties deteriorated due to obvious agglomerated submicron SiC particles as the volume fraction increased to 5% and 10%. On the contrary, for micron size SiC_p/AZ91 composite, the grain size was refined and the strengthening effect was enhanced with the increasing volume fraction. Although particle size has no influence on the texture type, it has different effects on weakening the intensity of texture.

Shen et al. (2014) investigated magnesium matrix composites reinforced with three volume fractions (3, 5 and 10 vol.%) of submicron-SiC particles ($\sim 0.5\mu\text{m}$) fabricated by semi-solid stirring assisted ultrasonic vibration method. With increasing volume fraction of the submicron SiC particles (SiC_p), the grain size of the matrix in the $\text{SiC}_p/\text{AZ31B}$ composites gradually decreased. Most of the submicron SiC particles exhibited homogeneous distribution in the $\text{SiC}_p/\text{AZ31B}$ composites. The ultimate tensile strength and yield strength of the 10 vol.% $\text{SiC}_p/\text{AZ31B}$ composites also improved. Study of the interface between the submicron SiC_p and the matrix in the $\text{SiC}_p/\text{AZ31B}$ composite suggested that submicron SiC_p bonded well with the matrix without interfacial activity.

Tiwari et al. (2007) investigated the corrosion behavior of two SiC reinforced Mg-based metal matrix composites, Mg-6SiC and Mg-16SiC (in volume percent), in freely aerated 1M NaCl solution and compared with that of pure Mg. The presence of SiC particles deteriorated the corrosion resistance of magnesium. Corrosion resistance decreased with increasing SiC volume fraction. The galvanic corrosion current density between pure SiC and pure Mg has been experimentally measured using zero resistance ammeter technique and theoretically determined using mixed potential theory. Galvanic corrosion between Mg matrix and SiC reinforcement in the composites did not contribute significantly to the overall corrosion rate. Electrochemical impedance spectroscopy indicated that the higher corrosion rates for the composites could be related to the defective nature of the surface film. Analysis of the surface scales after immersion in NaCl solution by microscopy and XRD analysis indicated that the surface films were similar in nature even with incorporation of SiC in Mg. Electrochemical impedance spectroscopy indicated that the higher corrosion rates for the composites may be related to the defective nature of the surface film. Fig. 2.12 shows typical SEM micrographs of (a) Mg and (b) Mg-6SiC surfaces obtained after immersion in 1M NaCl for 5 min.

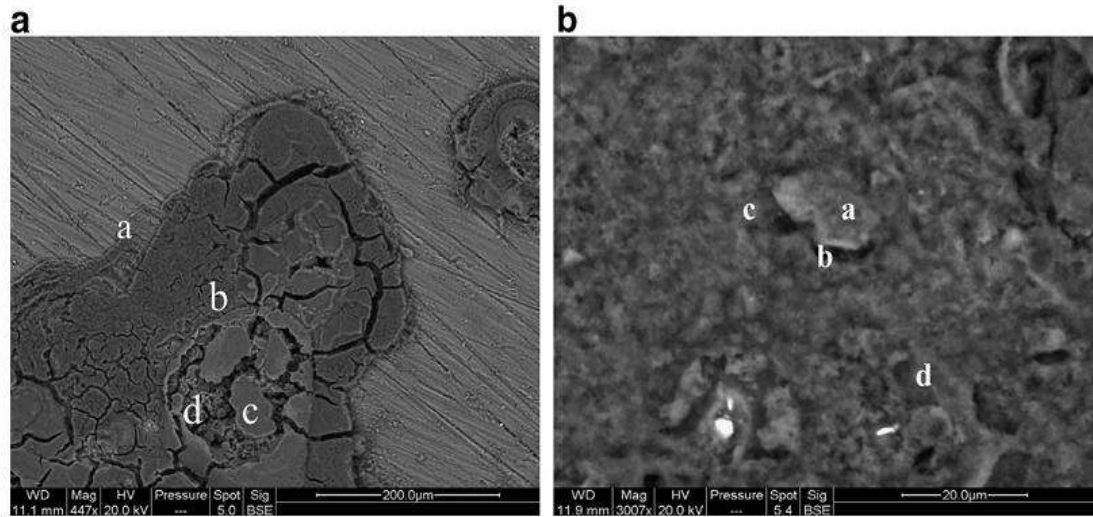


Fig. 2.12 Typical SEM micrographs of (a) Mg and (b) Mg–6SiC surfaces obtained after immersion in 1M NaCl for 5 min [Tiwari et al. (2007)]

2.5 Iron containing Composites

Konopka and Ozieblo (2001) studied metal reinforced ceramic composites ($\text{Al}_2\text{O}_3\text{-Fe}$) with various weight % of iron. The composites examined contained 10, 30 and 50 wt.% of Fe. Specimens were synthesized via wet-mixing using ethanol in an agate mill for 2 h. Isostatic compaction of the powder was done at a load of 120 MPa. Initial sintering was done at 900°C and final sintering at 1700°C in vacuum for 1.5 h. Fig. 2.13 shows SEM image of the microstructure of the $\text{Al}_2\text{O}_3 + \text{X}\%$ Fe composites showing the distribution of the FeAl_2O_4 spinel. FeAl_2O_4 spinel was identified in the microstructures of all the sintered samples. The distribution of the spinel can only be seen at higher magnifications. It forms during the sintering process at the metal–ceramic interface. The microstructure of the $\text{Al}_2\text{O}_3\text{-Fe}$ composites shows mostly spherical Fe particles distributed uniformly throughout the Al_2O_3 matrix. Because iron melts during sintering, its particle size in sintered samples differs from the starting particle size. The average Fe particle size after sintering is decreased. SEM studies revealed FeAl_2O_4 spinel phase which mostly had a granular morphology.

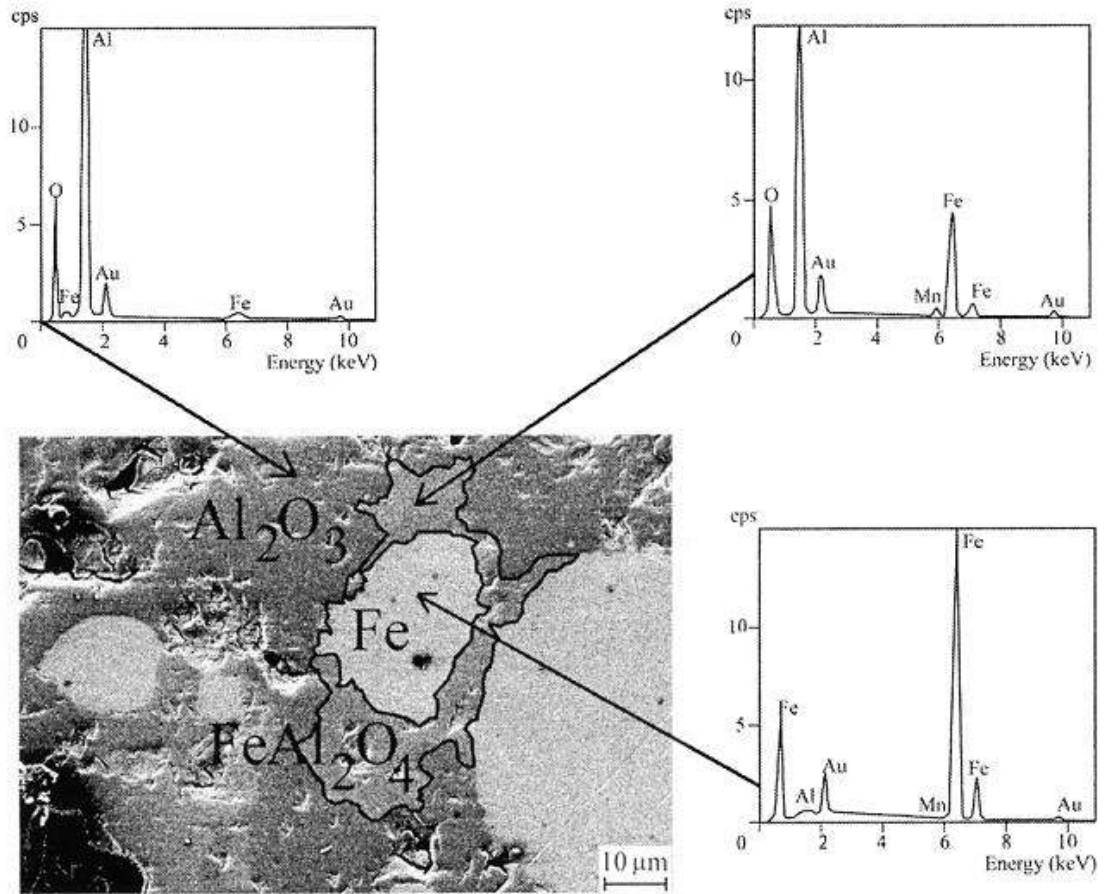


Fig. 2.13 SEM image of the microstructure of $\text{Al}_2\text{O}_3 + X\%$ Fe composites showing the distribution of the FeAl_2O_4 spinel [Konopka and Ozieblo (2001)]

Konopka and Ozieblo (2001) also reported the mechanical properties of Al_2O_3 -Fe composites with various weight % of iron. The fracture toughness (K_{IC}) of these composites was also measured. The K_{IC} depends on the Fe content in matrix and is limited by FeAl_2O_4 spinel formed in the composite during sintering. As the Fe content in the composite increases to 50wt. %, its hardness decreases and its fracture toughness increases with respect to that of the pure Al_2O_3 specimen. On the other hand, the composite composed of 50 wt.% Fe and 50 wt.% Al_2O_3 has the lowest value of K_{IC} of all the samples. These results indicate that Fe introduced into the Al_2O_3 matrix decreases the modulus E, and hence affects the value of K_{IC} .

Two mechanical properties which are of interest in relation to metal matrix composites are hardness and compressive strength. Zuhailawati et al. (2010) reported the mechanical alloying of iron-carbon (Fe-C) powders for various milling duration (2, 4, 6 and 8 h) and with different carbon content (1, 2, 3 and 4 wt.%). The milled powders were consolidated by cold pressing at 400 MPa and sintering at 1150°C. The sintered samples were examined under an optical microscope and a scanning electron microscope for study of the microstructure evolution and to measure density, Rockwell F and Vickers hardness. This technique has produced Fe-C alloy with pearlite structure at lower temperature as compared to the conventional technique. With increasing milling time, more pearlite formed which improved the hardness. Milling beyond 6 h, however, decreased the hardness due to the presence of higher porosity because hardened powder hindered densification. Similarly, the hardness value reached the maximum at 2% carbon before decreasing at 3% and 4% carbon levels due to the residual graphite.

Chang et al. (2010) reported iron-containing Hydroxyapatite/titanium composite via pressure less sintering at a relatively low temperature with particular emphasis on identifying the underlying toughening mechanisms. The addition of iron to HA/titanium composites led to a unique and favorable core/shell microstructure of Ti-Fe particles that consisted of titanium as shell and iron as core. This had good interfacial bonding with HA matrix. While the relative density, hardness and Young's modulus decreased, the flexural strength, fracture toughness, fatigue resistance, and the related fracture surface roughness increased significantly with increasing amount of Ti-Fe particles. Different toughening mechanisms including crack bridging, branching and deflection were observed in the composites. This effectively increased the crack propagation resistance and resulted in a substantial improvement in the mechanical properties of the composites.

Ramesh and Srinivas (2009) et al. investigated iron-silicon carbide metal matrix composites synthesized via direct metal laser sintering technology. Different powder mixtures were prepared with 1, 2, 3, 5 and 7wt. % of nickel-coated silicon carbide

with iron powder. Laser power was maintained constant at 180 W with laser beam diameter of 0.4 mm. Laser sintering scan speeds of 50, 75, 100 and 125 mm/s in steps of 25 were adopted while hatch spacing, hatch width and layer thickness were maintained constant at 0.2 mm, 5 mm and 50 μm respectively. Metallographic studies, friction and wear test using pin-on-disc were carried out on both the matrix metal and its composites. Load was varied from 10 to 80N while sliding velocity was varied from 0.42 to 3.36 m/s for 30min. It was found that the increased content of SiC in iron matrix resulted in significant improvement of both hardness and wear resistance. Lower the sintering speed, higher is the hardness and wear resistance of both the metal matrix and its composites. However, coefficient of friction of composites increased with increasing SiC under identical test conditions. SEM observations of the worn surfaces have revealed extensive damage to the iron pins as compared with that of the composites. Fig. 2.14 shows SEM of worn surfaces at sliding velocity of 1.26 m/s and load of 20N. (a) Iron-sintered at 100 mm/s. (b) Iron–3wt. % SiC sintered at 100 mm/s. It was found that the onset of adhesive process such as scuffing and seizure are restricted by increase in hardness of materials.

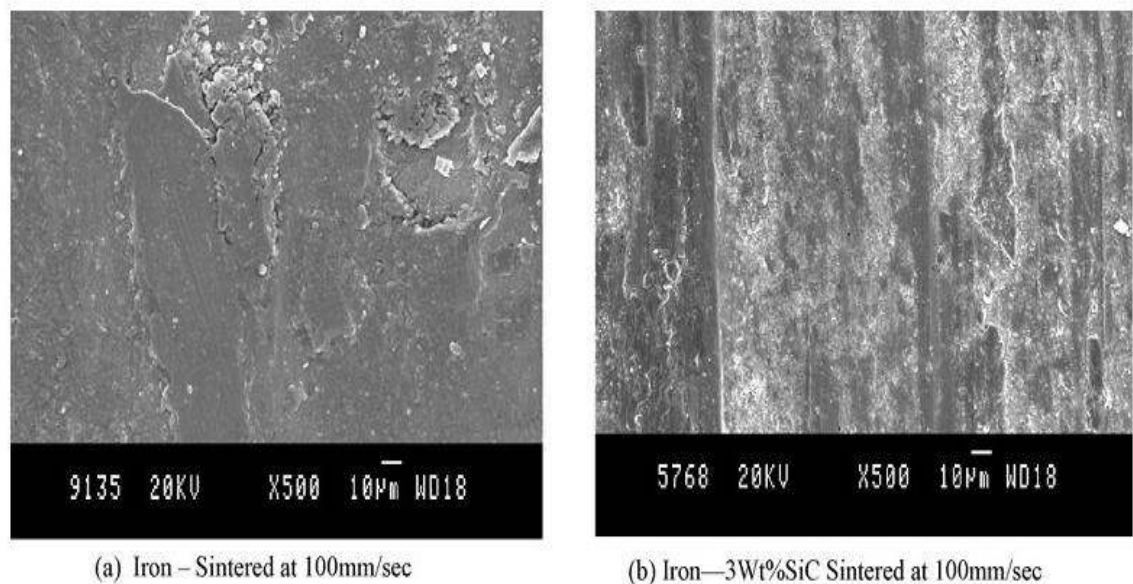


Fig. 2.14 SEM of worn surfaces at sliding velocity of 1.26m/s and load of 20N (a) Iron-sintered at 100 mm/s (b) Iron–3wt.% SiC sintered at 100 mm/s [Ramesh and Srinivas (2009)]

Sozhamannan et al. (2010) analysed the microstructure of random and clustered particles to determine its effect on the strength and failure mechanisms. The finite element analysis models were generated in ANSYS using scanning electron microscope images. Percentage of the major failures and stress–strain responses were predicted numerically for each microstructure. It is evident from the analysis that the clustering nature of particles in the matrix dominates the failure modes of particle reinforced metal matrix composites. The initial plasticity, which is due to decohesion of the interface at the matrix/particle region, decreases the load sharing capability, resulting in a decrease in the ultimate strength. In addition, the same phenomenon is observed for the particle clustering structure. The larger dimension of the particle is easily fractured due to the large stress concentration and high strain hardening rate around the particles and increased area of contact. The plastic deformation is initiated by the particle fracture and interface decohesion. The plastic constrain increased with an increase in the volume of the particle. Particle fracture, interface decohesion, volume fraction and size of particles, dominate the failure of PRMMCs.

In order to investigate the role of amorphous SiO₂ particles on the corrosion and wear resistance of Ni-based metal matrix composite alloying layer, amorphous nano-SiO₂ particles reinforced Ni-based composite alloying layer has been prepared by double glow plasma alloying on AISI 316L stainless steel surface, where Ni/amorphous nano-SiO₂ was pre-deposited by brush plating [Xu et al. (2008)]. The composition and microstructure of the nano SiO₂ particles reinforced Ni-based composite alloying layer were analyzed by using SEM, TEM and XRD. The results indicated that the composite alloying layer consisted of g-phase and amorphous nano-SiO₂ particles and under alloying temperature (1000°C) condition, the nano-SiO₂ particles were uniformly distributed in the alloying layer and still maintained the amorphous structure. The corrosion resistance of composite alloying layer was investigated by an electrochemical method in 3.5% NaCl solution. Compared with single alloying layer, the amorphous nano-SiO₂ particles slightly decreased the corrosion resistance of the Ni–Cr–Mo–Cu alloying layer. X-ray photoelectron spectroscopy (XPS) revealed that the passive films formed on the composite alloying consisted of Cr₂O₃, MoO₃, SiO₂

and metallic Ni and Mo. Fig. 2.15 shows SEM micrographs of corroded surfaces before and after anodic polarization curve tests in 3.5% NaCl solution: (a) original surface morphology of composite A; (b) corroded surfaces morphology of composite A. Results of dry wear test showed that the composite alloying layer had excellent friction-reduced property and the wear weight loss of composite alloying layer was less than 60% of that of Ni–Cr–Mo–Cu alloying layer.

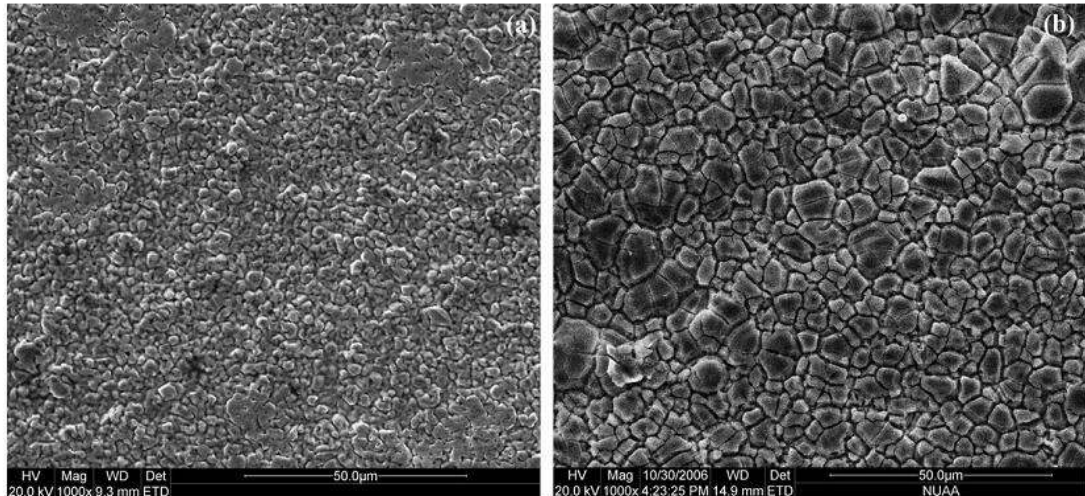


Fig. 2.15 SEM micrographs of corroded surfaces before and after anodic polarization curve tests in 3.5% NaCl solution: (a) original surface morphology of composite A; (b) corroded surfaces morphology of composite A [Xu et al. (2008)]

2.6 Motivation for Present Investigation

Significant work has been done using aluminium, magnesium and copper as the matrix materials with alumina, silicon carbide and tungsten carbide as reinforcement materials. These composites are used in light weight applications. For heavy duty applications, composites based on heavy metals such as iron, nickel or their alloys must be developed. Literature search done by us did not show any significant and systematic attempts for the study on the composites with iron as the matrix material. It prompted us to study and develop composite material with iron as the matrix metal. In the initial exploratory work it was found that iron-alumina metal matrix composites showed superior mechanical properties such as hardness and wear. On the basis of the results of the initial work, in the present investigation a detailed work was planned to

prepare Fe – Al₂O₃ Metal Matrix Composites by varying the percentage of Al₂O₃ and the processing parameters and characterizing the prepared specimens for mechanical properties e.g. hardness, wear and deformation and electrochemical properties; corrosion. Investigations were also planned to prepare and characterize hybrid Fe – Al₂O₃ – ZrO₂ composites and study the effect of doping of some metal oxides; CoO and CeO₂.

It is expected that the contents in the present chapter on literature review will prove to be helpful in understanding the research work undertaken by various researchers in the field of MMCs. It also helped me in finding the existing knowledge gaps in the processing of MMCs and thus guides in formulating the present research problem.

The next chapter 3: Aims and Objectives of the present work provide a detailed account of the aims and objectives of the present research work on MMNCs.